POLITECNICO
MILANO 1863

SCUOLA DI INGEGNERIA INDUSTRIALE
E DELL'INFORMAZIONE

EXECUTIVE SUMMARY OF THE THESIS

# Development of an algorithm for creating a digital model of trabecular bone

TESI MAGISTRALE IN BIOMEDICAL ENGINEERING – INGEGNERIA BIOMEDICA

**AUTHOR: GIACOMO GIORGETTI**

**ADVISOR: PASQUALE VENA**

**ACADEMIC YEAR: 2021-2022**

## 1. Introduction

Trabecular bone is found at the ends of long bones and in the middle of flat bones. Spongy bone is made up of elements called trabeculae that can be classified into two different types: plate-like and rod-like. Plate-like trabeculae are much smaller in one size than the other two, while rod-like are much larger in one size than the other two. Plate-like trabeculae represent the primary load-bearing component of the structure, while rod-like trabeculae have a load-dissipating and stabilizing function. In diseases such as osteoporosis, in addition to a deterioration of the micro-architecture of bone tissue, and consequent decreasing in mass, a progressive shift from plate-like to rod-like trabeculae has been observed [1].
The objective of this thesis is to develop a numerical tool capable of reproducing a digital cubic specimen of trabecular bone. By varying the input parameters, it will be possible to control the morphometric and mechanical parameters of the developed specimens, which can simulate both healthy and osteoporotic trabecular bone.

## 2. Algorithm for architecture generation

The algorithm for creating the models was developed in Matlab. The aim of the numerical tool is to obtain a trabecular structure with a prescribed ratio of rod-like to plate-like trabeculae. This is achieved making use of the 3D Voronoi tessellation of a cubic domain.

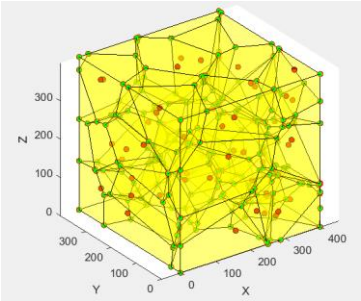


Figure 1: Cubic Voronoi tessellation with 50 seed-points

Initially, a cubic volume of interest (VOI) was defined in which seed-points were randomly arranged. At this point, the function 'voronoi3d_cuboid' was used, which performs a Voronoi tessellation of the 3D cubic domain for a given set of input seed points and vertices of the

VOI [2]. The Voronoi tessellation results in a set of edges and plates which will be potential rod-like or plate-like trabeculae (Figure 1). A further process is applied in order to transform edges and plates into trabeculae. To carry out the processing, the following morphological characteristics of trabecular bone were considered:

- most of the trabeculae are arranged along the load directions [3];
- maximum four trabeculae meet each other at one point [4];
- in healthy bone there is a prevalence of plate-like trabeculae [1];
- the rod-like trabeculae show thinning in the central area [4].

The Voronoi tessellation showed that each vertex of the polyhedron had no more than four connections. In this thesis, the z-axis was considered as the loading direction. The edges and faces of the Voronoi polyhedra were saved or removed with different probabilities depending on whether they had an orientation close to or away from the z-axis. Structures with an orientation close to the axis were saved with higher probability. Once the desired geometry was obtained, the saved edges and faces were assigned pixels to obtain a 3D image of the model. For the edges, more pixels were assigned to the ends with respect to the center in order to comply with the morphological character observed in the literature [4]. The final structure was expanded and finally a Gauss filter was applied to smooth the model. To perform morphometric and mechanical analyses, the digital specimens were transformed into binarized micro-CT-like images by taking 400 sections along the z-axis. To control the morphometric and mechanical parameters of interest, a few input parameters were used within the code:

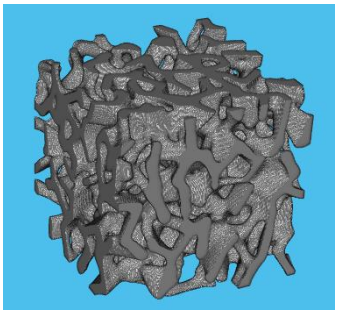

Figure 2: Example of final model

- number of seeds to be distributed randomly within the VOI ('N° seed');
- ratio between the number of rod-like and plate-like trabeculae ('N° rod-like/N° plate-like');
- dilation ('Radius')
- control of model anisotropy ('δ anisotropy').

The parameter δ anisotropy allows us to control the probability with which edges and faces are saved or removed. This parameter increases by a $\delta$ factor the probability assigned to edges and faces with probability greater than 0.6, while decreasing by a $\delta$ factor the elements with probability less than 0.6. For a digital model meant to reproduce a healthy bone specimen, the following input ranges were chosen because they were found to be the most suitable for creating these models:

- N° seed = 400 - 600
- N° *rod-like*/N° *plate-like* = 0.2 - 1
- Dilation → *strel('sphere', 6)*

In the dilation command, the number 6 corresponds to the radius value chosen to perform the dilation. For models meant to reproduce specimen of osteoporotic bone, the following input ranges were chosen because they were found to be the most suitable for creating these models:

- N° seed = 200 - 400
- N° *rod-like*/N° *plate-like* = 1 - 20
- Dilation → *strel('sphere', 5 or 6)*

In a healthy trabecular bone there is a higher bone density. For this reason, it was decided to use a higher number of seeds in healthy models. Regarding the ratio of rod-like to plate-like trabeculae, it can be seen that high values were chosen for the osteoporotic models (up to 20) as per observation in the literature [1]. The expansion applied to the two types of structures is quite similar as no excessive differences in thickness were noted between healthy and osteoporotic bone trabeculae. Moreover, two digital specimens were also created in order to change the direction of anisotropy to verify that we had control over the choice of loading direction. The two models were generated by setting the same input. For simplicity, the x-axis and y-axis were taken as references in the two specimens instead of the z-axis. Finally, two more models were created with the same inputs

but with random seed-points and ordered distribution (Figure 3).
111 models were generated in this thesis.

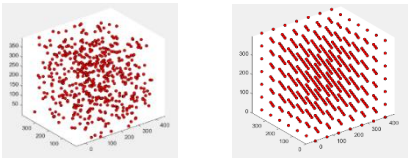

Figure 3: Random distribution of seed-points (left) and ordered distribution of seed-points (right)

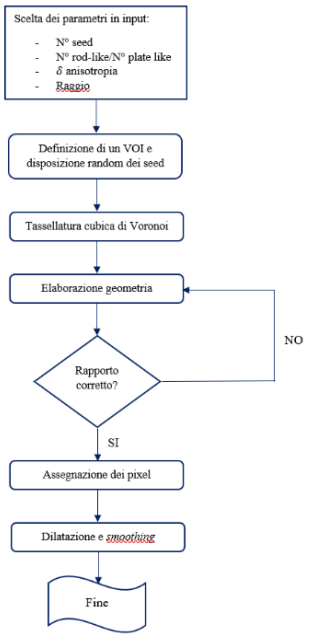


Figure 4: Block diagram of the model generation process

# 3. Analysis of models

## 3.1. Morphometric analysis

Morphometric analyses were performed with Fiji software using the BoneJ plug-in on all 111 generated models. The morphometric parameters that were analyzed are: volume fraction (BV/TV), thickness of trabeculae (TbTh), space between trabeculae (TbSp), degree of anisotropy (DA), Ellipsoid factor (EF) and Connectivity density (ConnD). The values for TbTh and TbSp returned by the software in pixels were converted to mm, and those for ConnD to $mm^{-3}$. A resolution of 0.01 mm/pixel was established for the conversion.

Considering all the models generated, the input ranges that were used are:

- N° seed = 189 – 800
- N° rod-like/N° plate-like = 0.2 – 20
- Radius = 1 - 10
- $\delta$ anisotropy = 0 – 0.45

After performing morphometric analyses of all specimens, we got the following ranges:

- BV/TV = 0.10 – 0.51
- TbTh (mm) = 0.11 – 0.45
- TbSp (mm) = 0.40 – 0.95
- DA = 0.16 – 0.55
- EF = -0.46 – 0.38
- ConnD ($mm^{-3}$) = 1.42 – 10.9

The input value ranges were always chosen with to obtain morphometric parameters compatible with those of a real trabecular bone.

## 3.2. Elastic mechanical analysis

The specimens were subjected to three uniaxial compressions along the Cartesian directions (x, y, z) and three shear stresses both confined (xy, yz, xz) to obtain the elastic and tangential elastic moduli normalized to the elastic modulus of the solid phase. The tests were carried out with ParOSol which is a parallel simulator that uses a voxel mesh given by the resolution of the images taken as input. To perform the simulations, the following inputs were set: elastic modulus (Es = 1 GPa) and Poisson's coefficient ($\upsilon$ = 0.3) of the solid phase, applied strain ($\varepsilon$ = 1) and specimen resolution (0.02 mm/pixel). For these tests, the specimen resolution was doubled to speed up the simulations.

## 3.3. Correlation analysis

Ten specimens were created for each input which were analyzed and varied in the specimens; while the others were kept fixed to obtain only the influence of the individual parameter in the results. Correlation analyses were performed on Excel. The morphometric analyses showed a strong positive correlation between N° seed and BV/TV (r = 0.93) and ConnD (r = 0.99) as expected. A strong correlation with EF (r = 0.92) was noted, probably because in the specimens with a high number of seeds the edges and faces of the Voronoi polyhedra

were shorter and had smaller areas, respectively. A moderate positive correlation between N° seed and TbTh (r = 0.80) was observed, due to more interconnections making the trabeculae thicker at those points. A small negative correlation with DA (r = 0.53), due to the randomness of the specimens, and a strong negative correlation with TbSp (r = - 0.97) as expected. For the input "N° rod-like/N° plate-like", a strong positive correlation with EF (r = 0.90) was noted as expected and a moderate negative correlation with ConnD (r = 0.73) and TbSp (r = 0.69) because rod-like trabeculae occupy a smaller volume and merge less than plate-like trabeculae during dilation. Finally, a moderate negative correlation was found with BV/TV (r = - 0.77) and no significant correlation with DA and TbTh. For the 'radius' input, strong positive correlations were obtained with BV/TV (r = 0.99) and TbTh (r = 0.995), while a strong negative correlation was obtained with TbSp (- 0.99). This is an expected result for both cases. Strong negative correlations were obtained for DA (r = - 0.92), EF (r = -0.99) and ConnD (r = - 0.89). For the DA, this result is because, as the expansion increases, the more material is added in all directions. For the EF, the reason lies in the fact that the plate-like trabeculae, initially non-dilated and in greater number, are smaller in size than the other two. Finally, for ConnD, the dilation could have led to the fusion of several trabeculae that are no longer detected by the software. As expected, the input "δ anisotropy" presents a strong positive correlation only with the DA (r = 0.94). It has no correlation with ConnD, TbSp and EF. It presents a strong negative correlation with TbTh (r = - 0.88) because, by increasing δ, there is a slight loss of trabeculae and therefore a probable lower interconnection that reduces the thickness of the structure at these points. It also shows a weak correlation with BV/TV (r = - 0.66) for the same reasons.

The elastic mechanical analyses showed a positive correlation between N° seed and elastic moduli as expected: r(Ex/Es) = 0.88, r(Ey/Es) = 0.81, r(Ez/Es) = 0.88, r(Gxy/Es) = 0.87, r(Gyz/Es) = 0.86 and r(Gxz/Es) = 0.86. Regarding the input 'rod-like/N° plate-like', a negative correlation emerged with all mechanical parameters: r(Ex/Es) = - 0.74, r(Ey/Es) = - 0.85, r(Ez/Es) = - 0.86, r(Gxy/Es) = - 0.86, r(Gyz/Es) = - 0.84 and r(Gxz/Es) = - 0.85. This result is also in line with the expected one as it reflects what has been observed in the literature [1]. For the "radius" input, strong positive correlations were obtained with all the mechanical parameters: r(Ex/Es) = 0.992, r(Ey/Es) = 0.993, r(Ez/Es) = 0.988, r(Gxy/Es) = 0.994, r(Gyz/Es) = 0.993 and r(Gxz/Es) = 0.991. Finally, for the input 'δ anisotropy', no correlation emerged with Ey, Ez, Gyz and Gxz. Instead, a negative correlation is present with Ex (r = - 0.79) and Gxy (r = - 0.80). In this case, one would have expected a higher positive correlation with the modulus in the z-direction. This is because trabeculae with an orientation other than the z-axis were more likely to be eliminated, making the structure more brittle even along this axis.

As a final analysis, the correlation between the BV/TV and the mechanical parameters was investigated as a strong influence of this parameter on the stiffness of the trabecular bone has been observed in the literature [5]. The results of the analysis showed a strong correlation with all mechanical parameters: r(Ex/Es) = 0.97, r(Ey/Es) = 0.96, r(Ez/Es) = 0.95, r(Gxy/Es) = 0.97, r(Gyz/Es) = 0.97 and r(Gxz/Es) = 0.97. Finally, the elastic modulus values obtained on the 39 specimens were compared with those obtained using models found in the literature that estimate the elastic modulus from the BV/TV considering the isotropic material. Looking at the results, the Roberts-Garboczi model is the one that best interpolates the results of the in-silico analysis with regard to the modulus in the x and y directions with a mean relative percentage error (MRPE) of 15.1% and 15.2% respectively. For the modulus in the z-direction, the best model is the Gibson-Ashby model with an MRPE of 13.3% (Figure 5).

Gibson–Ashby $$E = E_0\varphi^2$$

Roberts–Garboczi $$E = E_0\left(\frac{\varphi-\varphi_0}{1-\varphi_0}\right)^m,\ \varphi > 0.20$$
$$E = E_0 C\varphi^n,\ \varphi \leq 0.20$$

Figure 5: Roberts-Garboczi and Gibson-Ashby model equations. $\varphi$ is the volumetric fraction, while $E_0$ is the elastic modulus of the solid phase

# 4. Models

## 4.1. Models with different anisotropy

The morphometric analysis of the models obtained with different anisotropy directions (x and y) gave

very similar results since the input was the same. The mechanical analysis, which was only conducted for the model with anisotropy in the y-direction, confirms that the specimen is stiffer in the y-direction (Table 1).

Table 1: Ratios of elastic moduli along x, y and z

| | $E_x/E_y$ | $E_y/E_x$ | $E_z/E_x$ | $E_x/E_z$ | $E_z/E_y$ | $E_y/E_z$ |
|---|---|---|---|---|---|---|
| Model 55 | 0.784 | 1.275 | 0.963 | 1.038 | 0.775 | 1.324 |

## 4.2. Models with ordered and random seeds

Morphometric analysis showed the two specimens to have differences even though they were created using the same inputs.

Table 2: Morphometric parameters obtained from specimens with random distribution (model 83) and seed order (Model 82)

| MORPHOMETRIC PARAMETERS | | |
|---|---|---|
| | Model 82 (ordered) | Model 83 (random) |
| BV/TV | 0.48 | 0.42 |
| TbTh (mm) | 0.25 ± 0.04 | 0.29 ± 0.07 |
| TbSp (mm) | 0.40 ± 0.07 | 0.49 ± 0.19 |
| DA | 0.18 | 0.26 |
| EF | 0.04 | 0.04 |
| ConnD ($mm^{-3}$) | 6.26 | 5.11 |

Looking at Table 2, BV/TV and ConnD are higher for the ordered sample 82, while TbSp is lower. The reason for this is that an ordered distribution of seeds (Figure 3) leads to a pattern with more homogeneous pixels within the volume. Similarly, having a constant space between the seeds makes it more difficult to create disconnected parts of the structure which are then eliminated in the analysis, leading to a smaller number of remaining trabeculae with a higher TbSp. As far as DA is concerned, a lower value is found for the ordered model 82. This is due to the fact that the seeds, being arranged in an orderly manner, lead to a final model with trabeculae aligned along the three axes, decreasing the degree of anisotropy along the z-axis. Finally, looking at the TbTh, a higher value can be seen for the random specimen 83 because with a random distribution of the seeds there can be a higher density in certain parts of the volume leading to a greater trabecular thickness at those points (Figure 3). Table 3 shows the results obtained from the mechanical analysis.

Table 3: Mechanical parameters obtained from model 82 and 83

| MECHANICAL PARAMETERS | | | | | | |
|---|---|---|---|---|---|---|
| | $E_x/E_s$ | $E_y/E_s$ | $E_z/E_s$ | $G_{xy}/E_s$ | $G_{yz}/E_s$ | $G_{xz}/E_s$ |
| Model 82 | 0.173 | 0.165 | 0.216 | 0.039 | 0.044 | 0.042 |
| Model 83 | 0.143 | 0.135 | 0.173 | 0.028 | 0.033 | 0.038 |

Test specimen 82 (ordered) presents higher values for both elastic moduli and shear moduli. This result is undoubtedly related to the fact that sample 82 has a higher BV/TV. In this case, although the DA for sample 82 is lower, the mechanical anisotropy in the z-direction remains present.

## 4.3. Healthy and osteoporotic model

Table 4 shows the results of the morphometric analysis performed on a selected healthy (H) and osteoporotic (OP) specimen.

Table 4: Morphometric parameters obtained for the healthy model (model 40) and osteoporotic model (model 108)

| MORPHOMETRIC PARAMETERS | | | | | | |
|---|---|---|---|---|---|---|
| | BV/TV | TbTh (mm) | TbSp (mm) | DA | EF | ConnD ($mm^{-3}$) |
| Model 40 (H) | 0.36 | 0.24 ± 0.05 | 0.50 ± 0.17 | 0.27 | -0.06 | 5.57 |
| Model 108 (OP) | 0.16 | 0.23 ± 0.04 | 0.78 ± 0.27 | 0.26 | 0.27 | 2.64 |

Looking at the results, the BV/TV is higher for the healthy specimen. This result is in line with studies found in the literature [5]. It can also be seen that the TbTh is slightly lower for the osteoporotic specimen. In fact, small differences in trabecular thickness between healthy and osteoporotic bone specimens have been found in the literature. As

expected, higher values for TbSp are noted for the healthy specimen. Osteoporotic bone, in fact, has a lower density, leading to a larger trabecular space. Looking at the DA, almost equal values are obtained for the two models. Moreover, the δ anisotropy parameter was set equal to zero for both types of specimens. This is because a link between this morphometric parameter and osteoporosis has not been observed in the literature. Regarding EF, however, an important difference between the two models is noted. As mentioned above, some studies have found that osteoporosis leads to a gradual transition from plate-like to rod-like trabeculae [1]. Finally, as expected, ConnD is greater for the healthy specimen. In osteoporotic bone, a loss of bone material leading to a decrease in the number of trabeculae was observed. Table 5 shows the results of the elastic mechanical analysis.

Table 5: Mechanical parameters obtained for the healthy model (model 40) and osteoporotic model (model 108)

| MECHANICAL PARAMETERS | | | | | | |
|---|---|---|---|---|---|---|
| | $E_x/E_s$ | $E_y/E_s$ | $E_z/E_s$ | $G_{xy}/E_s$ | $G_{yz}/E_s$ | $G_{xz}/E_s$ |
| Model 40 (H) | 0.087 | 0.099 | 0.119 | 0.022 | 0.025 | 0.025 |
| Model 108 (OP) | 0.006 | 0.008 | 0.015 | 0.004 | 0.005 | 0.006 |

Looking at the results, a higher stiffness can be seen in the healthy specimen, as expected. In fact, a higher BV/TV and a much lower EF were obtained for this specimen. It can also be seen that the mechanical anisotropy in the z-direction was maintained for both models. Furthermore, as with the other specimens, very similar elastic modulus values in the x and y-direction are observed. Ultimately, the four healthy and osteoporotic specimens were compared both morphometrically and mechanically with human trabecular bone from different body districts. Assuming a solid phase elastic modulus of 18 GPa, both healthy and osteoporotic models were compatible with the values found for trabecular bone of the femoral head.

## 5. Conclusions

The aim of this thesis is to develop an algorithm capable of generating a digital trabecular bone specimen by controlling both morphometric and mechanical parameters. From the results of the correlation analysis, the input N° seed and radius have a great influence from both a structural and mechanical point of view. The parameter N° rod-like/N° plate-like allows us to control the type of trabeculae that will be predominant in the final model and to have a control over the stiffness of the specimens. The δ anisotropy parameter seems to be able to control the degree of anisotropy of the models. From a mechanical point of view, however, it does not appear to increase the stiffness along the direction of anisotropy imposed in the algorithm. This aspect could be improved by increasing the probability of the trabeculae that have an orientation along the loading direction, without decreasing the probability for the others. With the same input, good repeatability of the models was observed from both a morphometric and mechanical point of view. The algorithm could be used both for the design of scaffolds for bone tissue engineering and for the prediction of fracture risk associated with the patient's clinical condition by means of numerical simulations.

## Bibliography

[1] D. Porrelli *et al.*, "Trabecular bone porosity and pore size distribution in osteoporotic patients – A low field nuclear magnetic resonance and microcomputed tomography investigation," *J. Mech. Behav. Biomed. Mater.*, vol. 125, Jan. 2022.

[2] "3D_voronoi_cuboid_bounded - File Exchange - MATLAB Central." [Online]. Available: https://it.mathworks.com/matlabcentral/fileexchange/74742-3d_voronoi_cuboid_bounded. [Accessed: 14-Nov-2022].

[3] D. Chappard, M. F. Baslé, E. Legrand, and M. Audran, "Trabecular bone microarchitecture: A review," *Morphologie*, vol. 92, no. 299, pp. 162–170, Dec. 2008.

[4] X. Xu, "3D DIGITAL METHODS FOR QUANTITATIVE CT-BASED TRABECULAR VERTEBRAL BONE TEXTURE AND MICROARCHITECTURE ANALYSIS FOR FRACTURE RISK," 2020.

[5] A. A. Nazarian Dietrich von Stechow AE David Zurakowski AE Ralph Mü ller AE

Brian D Snyder, A. D. Nazarian Á von Stechow Á B D Snyder, A. Nazarian, R. Müller, D. B. Zurakowski Á D Snyder, and B. D. Snyder, "Bone Volume Fraction Explains the Variation in Strength and Stiffness of Cancellous Bone Affected by Metastatic Cancer and Osteoporosis," *Calcif Tissue Int*, vol. 83, pp. 368–379, 2008.

## 6. Acknowledgements

I would like to thank Professor Pasquale Vena for assigning me a very interesting project and for always being available and present during my thesis work. I would also like to thank the researcher Luca D'Andrea for following me in the final phase of the work, giving me valuable advice. Both were always prompt in answering questions and clarifying any doubts I had.

I also want to thank my parents and my sister for always supporting me in my choices and for always being there for me. Finally, I want to thank my girlfriend with whom I shared this journey, who was always by my side in the most difficult moments.